An Analysis of the Mechanism of Orthogonal Cutting

By

Keiji OKUSHIMA and Katsundo HITOMI

Department of Mechanical Engineering

(Received February 28, 1958)

Abstract

The orthogonal cutting mechanism with the transitional deformation range (i. e the "flow region" which exists between the rigid region of workpiece and the plastic region of steady chip), instead of the conventional shear plane, is analyzed theoretically in the case in which simple continuous chip is produced under the assumption of a perfectly plastic solid. Using the results, the experimental data for lead and brass are discussed.

The theoretical expressions derived thereby can be reasonably applied to a wide range of cutting conditions, and also to the cases associated with quasi-continuous and discontinuous types of chip without any contradiction. In all cases the starting boundary-line of flow region is situated under the conventional shear line, and the ending boundary-line above it.

The inclination angles of both boundary-lines and the sector angle of flow region increase with rake angle. With an increase of depth of cut, the inclination angle of starting boundary-line increases, while that of ending boundary-line and, hence, the sector angle increase for lead, but decrease for brass.

Furthermore, the strain of chip based on the cutting state with a flow region is much smaller than the conventional shear strain based on the cutting state with a single shear plane. The strain of chip decreases with an increase of rake angle, and it has a tendency to decrease slightly for lead and increase gradually for brass with an increase of depth of cut.

1. Introduction

On the theoretical analysis of the mechanism of orthogonal cutting associated with a simple continuous chip, it has been generally assumed that the chip formation is a process of shear (no fracture) confined to a single plane, i. e. the "shear plane", extending from the tip of tool to the sharp intersection of the free surfaces of workpiece

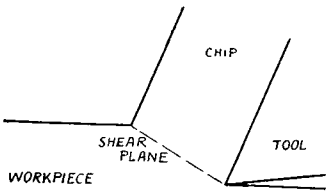

Fig. 1. The Cutting Process in the Conventional Theories.

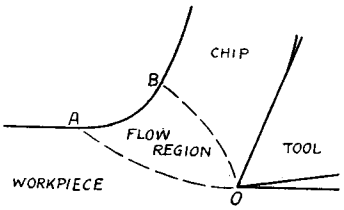

Fig. 2. The Cutting Process with the Flow Region.

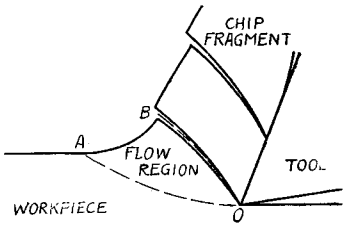

Fig. 3. The Discontinuous Chip Formation with the Flow Region.

and chip as shown in Fig. 1. The authors, however, pointed out in the previous paper[1]* that there are some weaknesses in the above process of chip removal and, in the strict analysis of metal cutting, the considerably wide transitional range of deformation AOB (called the "flow region") should be taken into consideration between the rigid region of workpiece and the plastic region of chip in steady state, as shown in Fig. 2, in order to get rid of weaknesses of an infinite acceleration which a moving metal-particle undergoes, an abrupt large strain and a large stress gradient on the single conventional shear plane.

Moreover, the formation of a discontinuous chip is also associated with the flow region; that is, as shown in Fig. 3, plastic deformation begins to occur at the starting boundary-line OA, plastic strain increases gradually with progress of cutting and ultimately exceeds the shearing breaking limit, at which instant fracture occurs at the ending boundary-line OB and one chip fragment is produced. It is considered, therefore, that a continuous chip is produced if the shearing stress or strain does not reach the breaking limit even at the ending boundary-line of flow region.

The present paper deals with the theoretical analysis of the mechanism of orthogonal cutting based on the flow region concept, and the data obtained with orthogonal dry cutting of such materials as lead and brass which produce a simple continuous chip are discussed.

2. The Analysis of the Mechanism of Orthogonal Cutting Based on the Flow Region Concept

a. The Situation of the Starting and Ending Boundary-Lines of Flow Region

In this section the cutting process, in which a continuous chip without built-up edge is produced, will be analyzed on the basis of the flow region concept.

It is assumed that the workpiece is of a perfectly plastic material and the elastic strain is negligible in comparison with the plastic strain as is often considered in

* Numbers in parentheses refer to the Bibliography at the end of the paper.

metal cutting. Then the shearing stress-strain relation ($\tau - \varepsilon$ diagram) becomes as shown in Fig. 4. In this figure τ_0 is the yield shearing stress, i. e. the shear-flow stress.

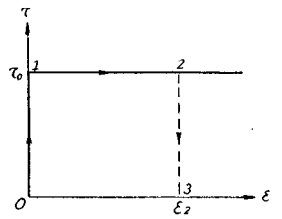

Fig. 4. Schematic Shearing Stress-Strain Diagram without Elastic Strain for a Perfectly Plastic Solid.

It is also assumed for the sake of simplicity that the starting (work side) and ending (chip side) boundary-lines of flow region are straight lines as shown in Fig. 5 (in reality, they are slightly convex downward and upward respectively). In this figure, the transitional flow shifting from the workpiece to

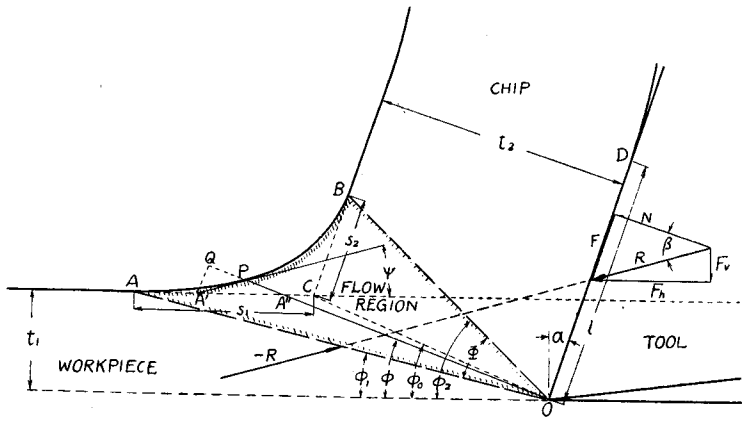

Fig. 5. Analysis of the Cutting Mechanism with the Flow Region.

the steady chip occurs in the flow region AOB and the stress in the flow region is in the yield state. Hence, on both boundary-lines,

$$\tau_{OA} = \tau_{OB} = \tau_0 . \tag{1}$$

Cutting with a depth of cut t_1 by the orthogonal cutting tool of rake angle α, the thickness of chip and the resultant cutting force (per unit width of cut) are supposed to be t_2 and R respectively. Then, under the assumption that the shearing stresses on both boundary-lines distribute uniformly, the following expressions are obtained:

$$\tau_{OA} = \frac{R \sin \phi_1 \cos (\phi_1 - \alpha + \beta)}{t_1} \tag{2}$$

and

$$\tau_{OB} = \frac{R \cos (\phi_2 - \alpha) \cos (\phi_2 - \alpha + \beta)}{t_2} , \tag{3}$$

where β is the mean friction angle on the tool face, and ϕ_1 and ϕ_2 are the inclination angles of starting and ending boundary-lines of flow region respectively.

It is known from recent reports[2,3] that the average tangential stress τ_{OD} on the tool-chip interface OD is in the yield state. Hence,

$$\tau_{OD} = \frac{R\sin\beta}{l} = \tau_0, \tag{4}$$

where l is the contact length of chip on the tool face.

The inclination angles of starting and ending boundary-lines of flow region ϕ_1 and ϕ_2 are derived explicitly from Eqs. (1) to (4) as follows:

$$\phi_1 = \frac{1}{2}\left[\alpha-\beta+\sin^{-1}\left\{\frac{2}{k_1}\sin\beta+\sin(\beta-\alpha)\right\}\right] \tag{5}$$

and

$$\phi_2 = \alpha-\frac{\beta}{2}+\frac{1}{2}\cos^{-1}\left(\frac{2}{k_2}\sin\beta-\cos\beta\right), \tag{6}$$

where k_1 is the ratio between contact length of chip and depth of cut, and k_2 is the ratio between contact length and thickness of chip.

$$k_1 = \frac{l}{t_1} \tag{7}$$

$$k_2 = \frac{l}{t_2} \tag{8}$$

Meyer-Archibald[4,5] and Creveling-Jordan-Thomsen[6] obtained

$$k_1 \approx 2 \quad \text{and} \quad k_2 \approx 1$$

respectively as the result of steel cutting. Consequently Eqs. (5) and (6) may be expressed as follows:

$$\phi_1 = \frac{1}{2}\left[\alpha-\beta+\sin^{-1}\left\{\sin\beta+\sin(\beta-\alpha)\right\}\right] \tag{5'}$$

and

$$\phi_2 = \alpha-\frac{\beta}{2}+\frac{1}{2}\cos^{-1}(2\sin\beta-\cos\beta). \tag{6'}$$

The sector angle of flow region $\varPhi$ is given by the difference between both angles obtained above, that is, from Eqs. (5) and (6)

$$\varPhi = \phi_2-\phi_1 = \frac{1}{2}\left[\alpha+\cos^{-1}\left(\frac{2}{k_2}\sin\beta-\cos\beta\right)-\sin^{-1}\left\{\frac{2}{k_1}\sin\beta+\sin(\beta-\alpha)\right\}\right]. \tag{9}$$

The mean friction angle on the tool face β used above is the arctangent of the friction coefficient μ acting between the sliding chip and the tool face, and is calculated with the following relation:

$$\mu = \tan\beta = \frac{F}{N} = \frac{F_v+F_h\tan\alpha}{F_h-F_v\tan\alpha}, \tag{10}$$

where F : tangential force component acting between tool face and chip
N : normal force component acting between tool face and chip
F_h : horizontal or principal cutting force
F_v : vertical or thrust cutting force.

There is an opinion[2,7] that Coulomb's rule of friction is not satisfied on the tool-chip interface and, consequently, the friction angle on the tool face is meaningless. However, since there is no established theory on the chip contact process, the mean friction coefficient μ, evaluated with the ratio between F and N, is used in the present paper. The friction angle β is a value always calculated as $\tan^{-1}\mu$. From this point of view there is no irrationality with respect to the mean friction angle β used in the above analytical expressions.

Putting a point at which the extended lines of free surfaces of the workpiece and of the chip cross one another as C, a straight line OC denotes the conventional shear plane. The lengths from the point C to starting and ending points of flow on the free surface A and B can be calculated with the following expressions:

$$s_1 = t_1\left(\cot\phi_1 - \frac{1-r\sin\alpha}{r\cos\alpha}\right) \tag{11}$$

and

$$s_2 = \frac{t_1}{\cos\alpha}\left\{\frac{\sin\phi_2}{r\cos(\phi_2-\alpha)} - 1\right\}, \tag{12}$$

where r is the cutting ratio.

$$r = \frac{t_1}{t_2} \tag{13}$$

b. The Plastic Shearing Strain in the Flow Region and the Strain of Chip

First of all let us determine the shearing strain on an arbitrary radial plane OP (ϕ denotes its inclination angle to cutting direction) extending from the cutting edge in the flow region. If the metal does not bring about the plastic deformation, a metal-particle on the free surface of the material uncut should proceed toward A''. But in reality it moves toward P as a result of plastic deformation, and has the motion component to $A'P$-direction (the tangent of the free surface of flow region at an arbitrary point P which makes the angle ψ to the machined surface), and so the shearing strain that the metal undergoes till it reaches the radial plane OP is given with $\frac{A''P}{A'Q}$ (where $A'Q$ is a perpendicular set on $A''P$), which is expressed by angles ϕ and ψ as follows:

$$\varepsilon = \cot\phi - \cot(\phi+\psi)\,. \tag{14}$$

In particular, the shearing strains on the starting and ending boundary-lines of flow region ε_1 and ε_2 are evaluated as follows:

$$\varepsilon_1 = 0 \tag{15}$$

and

$$\varepsilon_2 = \cot\phi_2 + \tan(\phi_2 - \alpha)\,. \tag{16}$$

The above leads to the conclusion that a large strain does not occur suddenly on a single boundary-line (the conventional shear plane) as it is the case in the conventional theories, but the shearing strain is zero on the starting boundary-line of flow region and increases gradually till it reaches maximum at the ending boundary-line of flow region. Then the metal enters into the chip region accompanying the permanent plastic strain ε_2. Whether such maximum value of shearing strain is under or above the breaking limit seems to determine the types of chip, continuous or discontinuous. Referring to Fig. 4, a metal-particle is at the position *0* in the workpiece, and is situated at the position *1* on the starting boundary-line of flow region, then it changes from the position *1* to the position *2* continuously in the flow region till it reaches the position *2* on the ending boundary-line, and, after entering into the chip region, it drops to the position *3* with the decrease of stress so that the permanent shearing strain ε_2 is left in the chip. This is the strain of chip and is given by Eq. (16).

3. Experimental Procedures

Orthogonal cutting was performed dry at a constant cutting velocity of 5.2 m/min and with various combinations of rake angle and depth of cut.

A shaper (Wakayama Iron Works Co.; stroke 19″) was used for the experiment.

Materials used were lead (Pb: 98.94%, Sn: 1.03%, Sb: 0.03%; Brinell hardness: 12 at 500 kg; width of cut: 11 mm, and length: 100 mm) and brass (Cu: 75.0%, Zn: 25.0%; Brinell hardness: 107 at 1000 kg; width of cut: 6 mm, and length: 70 mm), both of which easily produce a continuous chip without built-up edge under the usual cutting conditions.

The tool material was high speed steel SKH 2 (18–4–1), and the tool shape was sharp-edged with relief angle of 6° and various rake angles (i.e. −20°, −10°, 0°, 10° and 20°). The tools were finished with lapping by oil stone after grinding by diamond wheel.

Two components—principal and vertical— of cutting force were measured with the wire resistance type tool dynamometer[8].

After cutting, the contact length of chip on the tool face and the average thickness of chip were measured with the universal measuring microscope and the dial gauge respectively.

4. Experimental Results

In the case of lead cutting, the continuous chip without built-up edge was produced

and the machined surface was very smooth. On the other hand, in the case of brass cutting, the continuous chip without built-up edge was produced with comparatively smooth machined surface for positive rake angle and small depth of cut, but with large negative rake angle and/or an increase of depth of cut the chip often tended to produce the quasi-continuous type (which has periodical cracks at the back side which disappear midway to the separating side so that the chip is connected at the side of tool face) or to produce rarely the complete discontinuous type, on which occasion the cutting force changed periodically and the machined surface was associated with periodical chatter-marks.

The various cutting data for lead and brass are as follows:

a. The Influence of Rake Angle

Figs. 6 and 7 show the effect of rake angle upon the cutting force, the chip contact length and the chip thickness at cutting of lead (width of cut: 11 mm) and brass (width of cut: 6 mm) with depths of cut of 0.10 and 0.05 mm respectively at a constant cutting velocity of 5.2 m/min. It is evident from these figures that all quantities decrease with an increase of rake angle. In the case of brass cutting, the

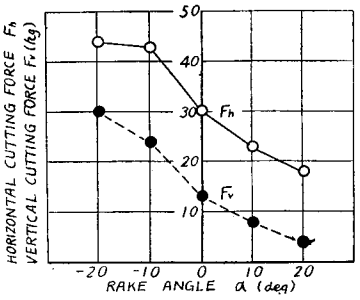

(a) Cutting Force (Width of Cut 11 mm)

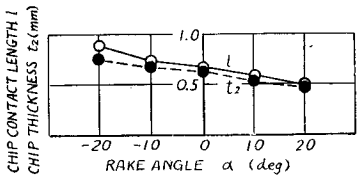

(b) Contact Length and Thickness of Chip

Fig. 6. Cutting Data for Lead in Relation to Rake Angle.

(Cutting Conditions: Cutting Velocity 5.2 m/min, Depth of Cut 0.10 mm)

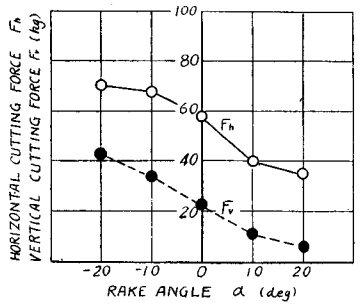

(a) Cutting Force (Width of Cut 6 mm)

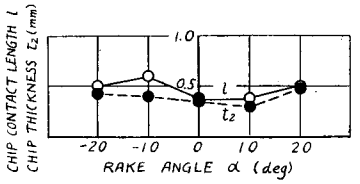

(b) Contact Length and Thickness of Chip

Fig. 7. Cutting Data for Brass in Relation to Rake Angle.

(Cutting Conditions: Cutting Velocity 5.2 m/min, Depth of Cut 0.05 mm)

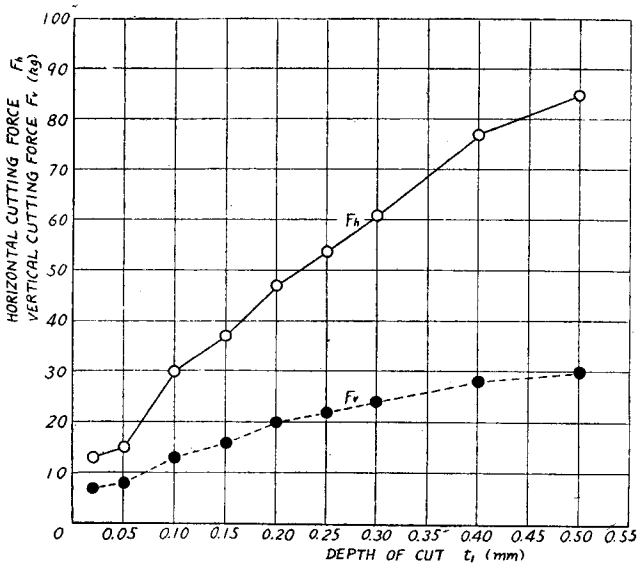

(a) Cutting Force (Width of Cut 11 mm)

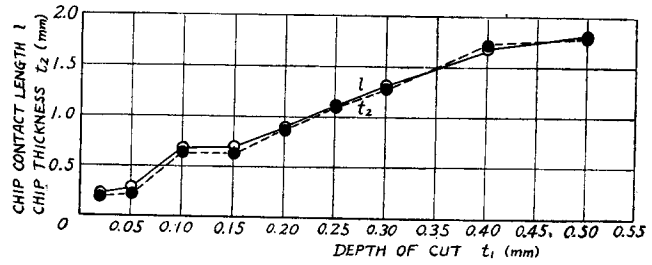

(b) Contact Length and Thickness of Chip

Fig. 8. Cutting Data for Lead in Relation to Depth of Cut.
(Cutting Conditions: Cutting Velocity 5.2 m/min
Rake Angle 0°)

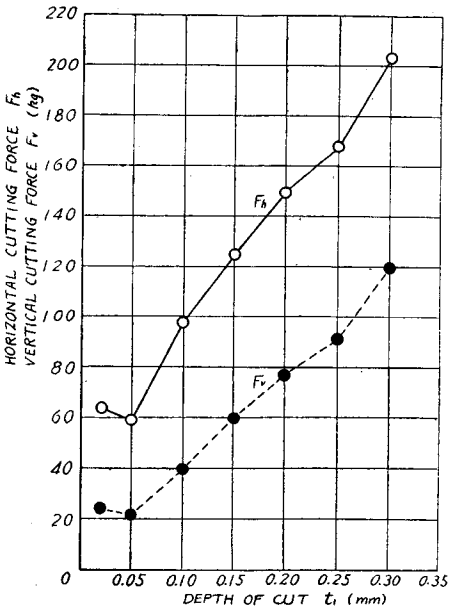

(a) Cutting Force (Width of Cut 6 mm)

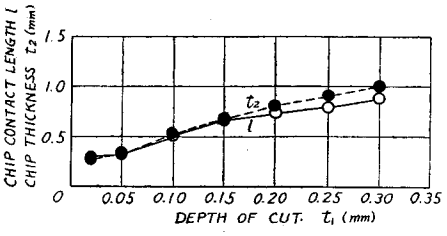

(b) Contact Length and Thickness of Chip

Fig. 9. Cutting Data for Brass in Relation to Depth of Cut.
(Cutting Conditions: Cutting Velocity 5.2 m/min
Rake Angle 0°)

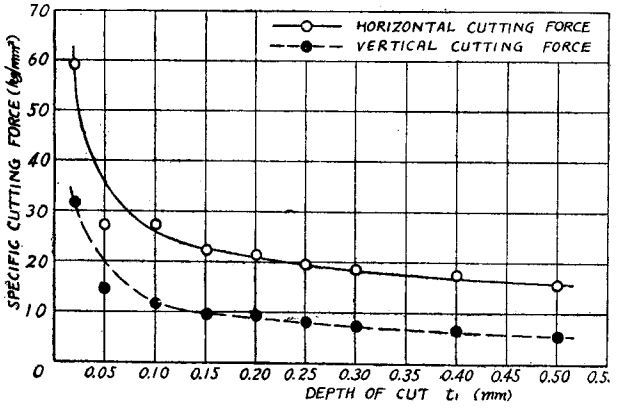

Fig. 10. The Specific Cutting Force in Relation to Depth of Cut in the Case of Lead.
(Cutting Conditions: Cutting Velocity 5.2 m/min
Rake Angle 0°)

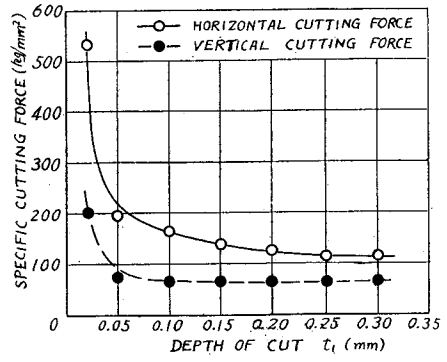

Fig. 11. The Specific Cutting Force in Relation to Depth of Cut in the Case of Brass.
(Cutting Conditions: Cutting Velocity 5.2 m/min
Rake Angle 0°)

quasi-continuous chip was produced at rake angle of $-20°$.

b. The Influence of Depth of Cut

Figs. 8 and 9 show the effect of depth of cut upon the cutting force, the chip contact length and the chip thickness at cutting of lead (width of cut: 11 mm) and brass (width of cut: 6 mm) with a tool of zero rake angle at a constant cutting velocity of 5.2 m/min. All quantities increase with depth of cut. In the case of brass cutting, at depths of cut of 0.15 and 0.20 mm the quasi-continuous chip or sometimes the complete discontinuous chip was produced.

Then the specific cutting force is calculated with the above data, and shown in Figs. 10 and 11. In both cases, with a decrease of depth of cut, the specific cutting force remains constant or increases very gradually in large depth of cut, and increases suddenly in small depth of cut; in other words, the size effect is recognized.

5. Discussions on the Mechanism of Orthogonal Cutting

The authors try to discuss the theoretical expressions derived on the basis of the cutting mechanism with a flow region by using the experimental data for lead and brass, and make a comparison with the results obtained by the conventional theory.

Lead has non-strain-hardening property at cutting performance because of its low recrystallization temperature and always produces a continuous chip without built-up edge; therefore, it is one of the most suitable materials to use for the analysis of metal cutting under the assumption of a perfectly plastic solid. On the other hand, brass sometimes produces quasi-continuous or discontinuous type of chip for negative rake angle and/or large depth of cut, but it produces continuous type of chip in the usual cutting conditions. Since the strain-hardening property of brass is not so small as that of lead, strictly speaking, the theoretical expressions cannot be applied on brass.

a. The Effect of Rake Angle

The calculated quantities by the experimental data in relation to rake angle (Figs. 6 and 7) are plotted in Fig. 12 for lead and Fig. 13 for brass.

The cutting ratio r, the ratio between contact length of chip and depth of cut k_1, and the ratio between contact length and thickness of chip k_2 are calculated with Eqs. (13), (7) and (8) respectively. With an increase of rake angle, r increases, k_2 is almost constant, and k_1 decreases for lead and varies irregularly for brass.

The mean friction angle on the tool face β, the inclination angles of starting and ending boundary-lines of flow region ϕ_1 and ϕ_2, and the sector angle of flow region $\varnothing$ are calculated with Eqs. (10), (5), (6) and (9) respectively. Further, in order to compare with ϕ_1 and ϕ_2, the conventional shear angle ϕ_0 based on the cutting mechanism with a single shear plane is obtained from the following expression by using a term

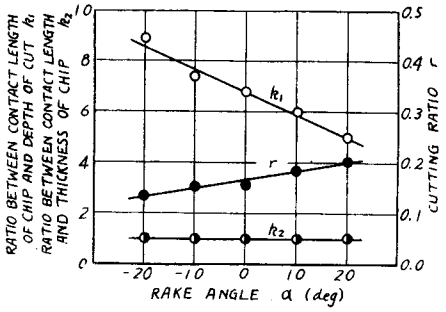

(a) Cutting Ratio, Ratio between Contact Length of Chip and Depth of Cut, and Ratio between Contact Length and Thickness of Chip

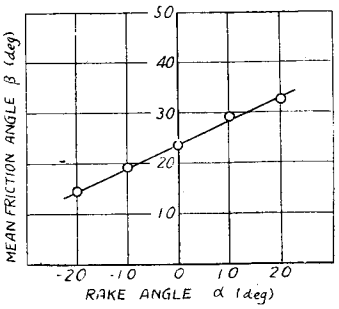

(b) Mean Friction Angle

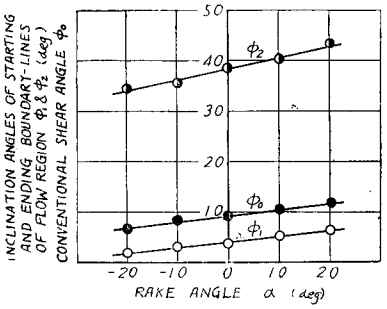

(c) Inclination Angles of Starting and Ending Boundary-Lines of Flow Region, and Conventional Shear Angle

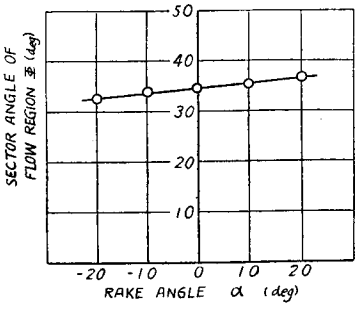

(d) Sector Angle of Flow Region

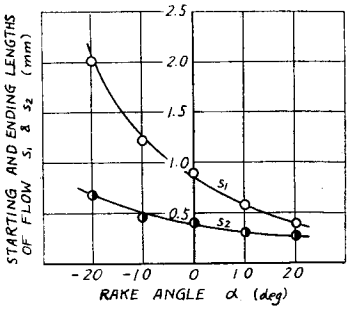

(e) Starting and Ending Lengths of Flow

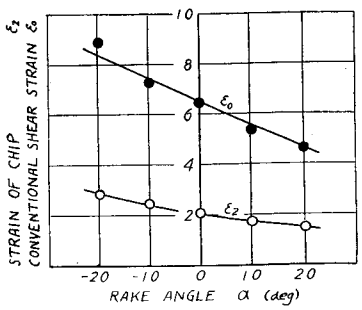

(f) Strain of Chip, and Conventional Shear Strain

Fig. 12. The Calculated Quantities for Lead in Relation to Rake Angle.
(Cutting Conditions: Cutting Velocity 5.2 m/min, Depth of Cut 0.10 mm)

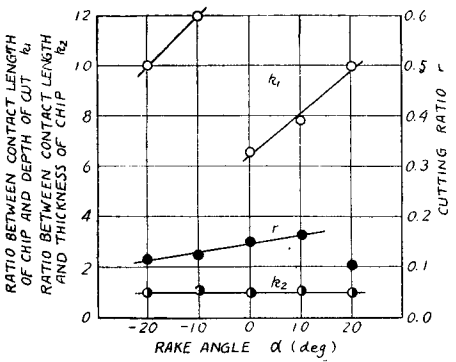

(a) Cutting Ratio, Ratio between Contact Length of Chip and Depth of Cut, and Ratio between Contact Length and Thickness of Chip

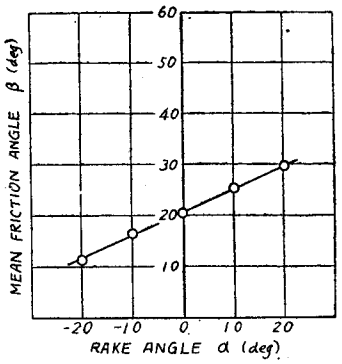

(b) Mean Friction Angle

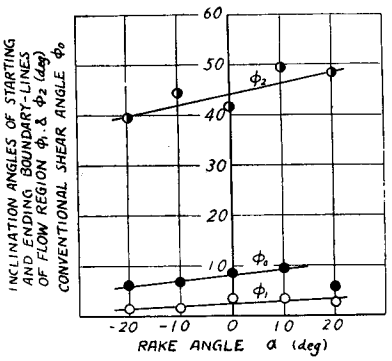

(c) Inclination Angles of Starting and Ending Boundary-Lines of Flow Region, and Conventional Shear Angle

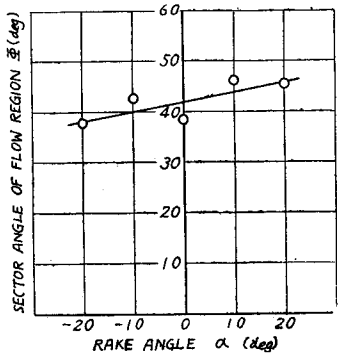

(d) Sector Angle of Flow Region

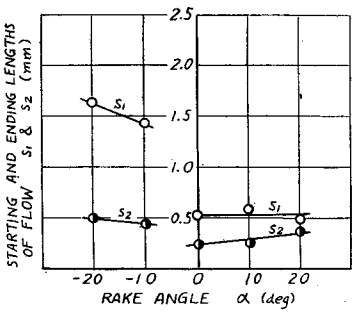

(e) Starting and Ending Lengths of Flow

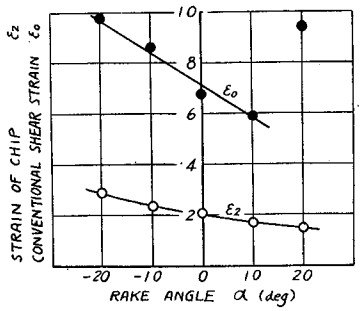

(f) Strain of Chip, and Conventional Shear Strain

Fig. 13. The Calculated Quantities for Brass in Relation to Rake Angle.
(Cutting Conditions: Cutting Velocity 5.2 m/min, Depth of Cut 0.05 mm)

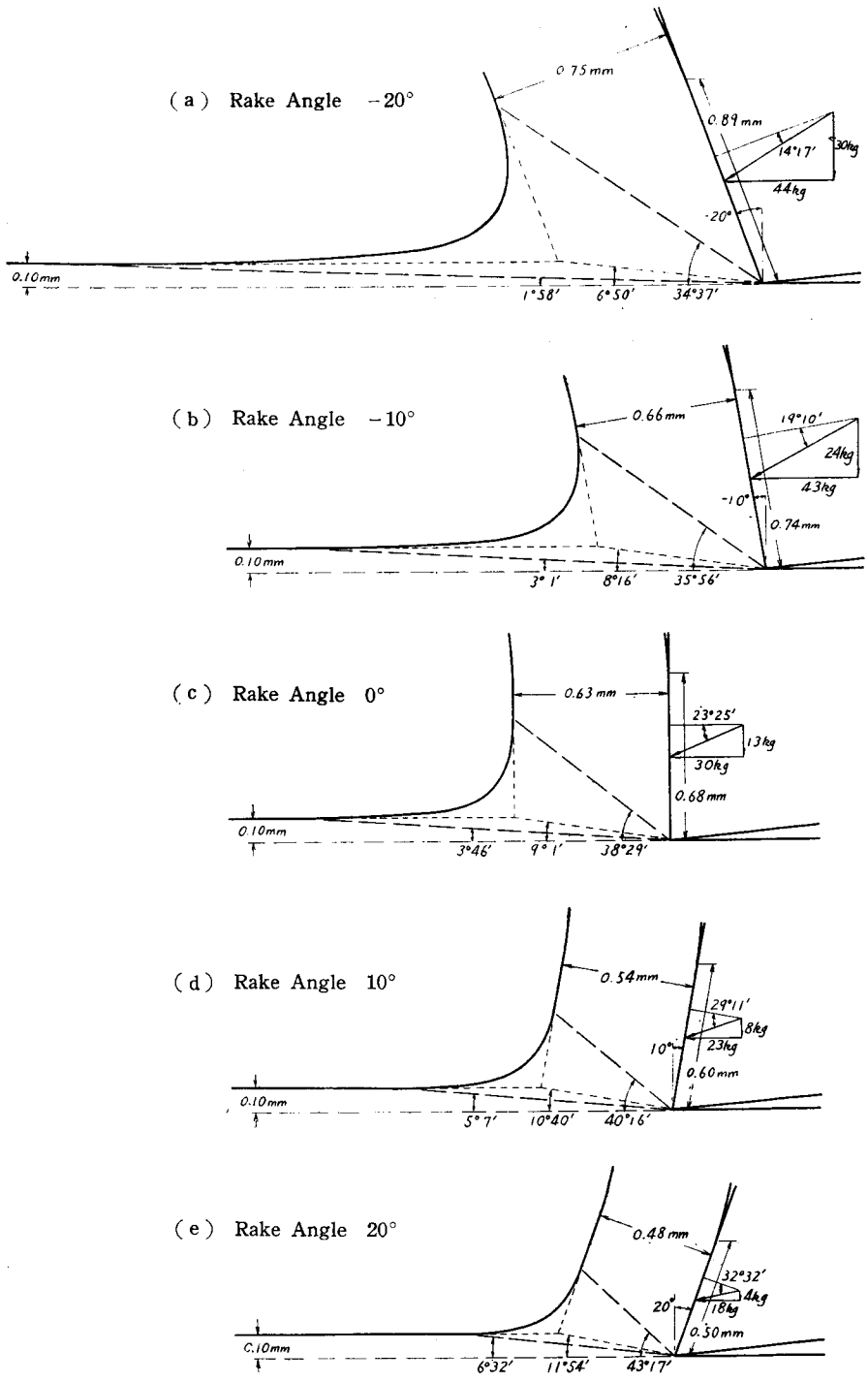

Fig. 14. The Cutting Schema for Lead in Relation to Rake Angle.
(Cutting Conditions: Cutting Velocity 5.2 m/min, Depth of Cut 0.10 mm)

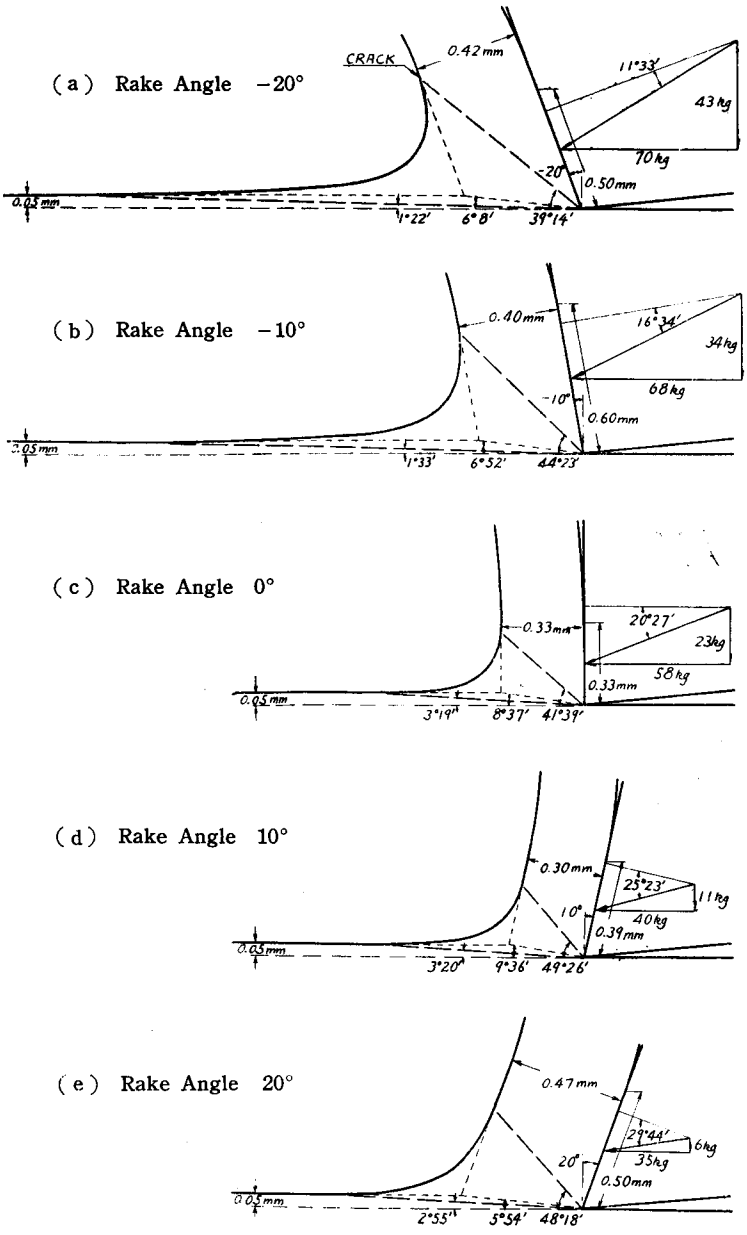

Fig. 15. The Cutting Schema for Brass in Relation to Rake Angle.
(Cutting Conditions: Cutting Velocity 5.2m/min, Depth of Cut 0.05mm)

of cutting ratio r, and it is also shown in Figs. 12 and 13 (c).

$$\phi_0 = \tan^{-1} \frac{r \cos \alpha}{1 - r \sin \alpha} \tag{17}$$

All quantities have a tendency to increase with an increase of rake angle for both lead and brass. The inclination angle of starting boundary-line of flow region ϕ_1 is always smaller than the conventional shear angle ϕ_0, and that of ending boundary-line ϕ_2 is larger, which means rationality of the concept discussed in Fig. 2. Such cutting schema drawn in relation to rake angle is shown in Fig. 14 for lead and Fig. 15 for brass. Observing from these figures, it is evident that the transitional deformation region between the workpiece and the chip is significantly wide and, further, its sector angle increases with rake angle. This goes to show the fact that larger rake angle insures smoother formation of chip. While the calculated values by the conventional theoretical equations of the shear angle derived by many investigators are not in accord with the observed values for negative rake angles, it is a noteworthy fact that the flow region concept expressed by Eqs. (5) and (6) gives very rational machining state even for large negative rake angles. Furthermore, the expressions are not inconsistent even when applied to the case of quasi-continuous chip which is contrary to the assumption [see Fig. 15 (a)]. It is supposed from this fact that the formation of quasi-continuous (and also discontinuous) types of chip also is associated with the flow region and crack occurs at the ending boundary-line of flow region because of excess stress and strain over the breaking limit as discussed in Fig. 3.

Further, the starting and ending lengths of flow s_1 and s_2 are calculated with Eqs. (11) and (12). In the case of lead these decrease with an increase of rake angle in spite of the increase tendency of the sector angle of flow region, while in the case of brass these have a tendency to decrease for negative rake angle and increase for positive rake angle (including zero rake angle) — which appears to have a bearing upon variation of the ratio between contact length of chip and depth of cut.

The strain of chip ε_2 is calculated with Eq. (16) and compared with the shear strain ε_0 based on the conventional cutting process with a single shear plane which is given by the following expression:

$$\varepsilon_0 = \cot \phi_0 + \tan (\phi_0 - \alpha) . \tag{18}$$

Both decrease with an increase of rake angle, but the strain of chip is much smaller than the conventional shear strain.

b. The Effect of Depth of Cut

The calculated quantities by experimental data in relation to depth of cut (Figs. 8 and 9) are plotted ni Fig. 16 for lead and Fig. 17 for brass.

With an increase of depth of cut, the cutting ratio r increases, the ratio between contact length of chip and depth of cut k_1 decreases, and the ratio between contact length and thickness of chip k_2 is almost constant. Referring to Figs. 12, 13, 16 and 17 (a), values of k_1 are in a wide range [3~15], much larger than the value [2] obtained by Meyer-Archibald[4,6], while the value of k_2 is nearly one [0.9~1.5] which is in accordance with the value obtained by Creveling-Jordan-Thomsen[6] in the case of steel cutting. This leads to the conclusion that the inclination angle of ending boundary-line of flow region ϕ_2 may be calculated tolerably accurately with Eq. (6′) instead of Eq. (6), while that of starting boundary-line ϕ_1 cannot be accurately determined from Eq. (5′).

The inclination angle of starting boundary-line of flow region ϕ_1 and the conventional shear angle ϕ_0 increase with depth of cut. The inclination angle of ending boundary-line ϕ_2 and, hence, the sector angle of flow region $\varnothing$ increase for lead, while they decrease for brass. This seems to have a connection with the decrease tendency of the mean friction angle on the tool face β for lead and its increase tendency for brass with an increase of depth of cut. Such inverse relationship between ϕ_2 and β can be explained by Eq. (6) since k_2 in the expression is a constant as described above. Again referring to Figs. 16 and 17, similarly as in the case where rake angle is changed, the inclination angle of starting boundary-line ϕ_1 is always smaller than the conventional shear angle ϕ_0 and that of ending boundary-line ϕ_2 is larger. The schema drawn for this case, therefore, becomes as shown in Fig. 18 for lead and Fig. 19 for brass. When brass was cut with depths of cut of 0.15 and 0.20 mm, the chip produced was quasi-continuous type or rarely discontinuous type. Even when applied to such case which is contrary to the assumption made in the analysis, the theoretical expressions are not inconsistent [see Fig. 19 (c) and (d)]—which makes possible the similar consideration as in the former paragraph.

Furthermore, in the case of lead the starting and ending lengths of flow s_1 and s_2 increase gradually with depth of cut because of the increase tendency of the sector angle of flow region, while in the case of brass these increase at small depth of cut and then decrease in spite of the simple decrease tendency of the sector angle. Referring to Figs. 12, 13, 16 and 17 (d) and (e), it is evident that the starting and ending lengths of flow do not necessarily show the same tendency of change as the sector angle of flow region associated with change of rake angle or depth of cut.

With an increase of depth of cut, the strain of chip ε_2 and the conventional shear strain ε_0 decrease slightly in the case of lead, while the strain of chip increases slightly and the conventional shear strain decreases in the case of brass. Referring to Figs. 12, 13, 16 and 17 (f), the conventional shear strain is always larger (about 1.2~6.8-fold) than the strain of chip. It appears from this fact that the strain rate

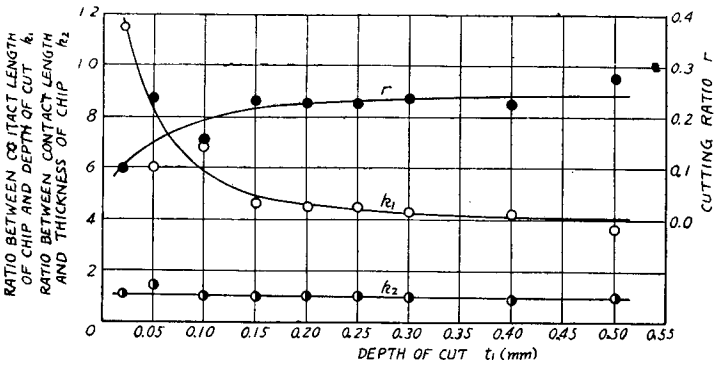

(a) Cutting Ratio, Ratio between Contact Length of Chip and Depth of Cut, and Ratio between Contact Length and Thickness of Chip

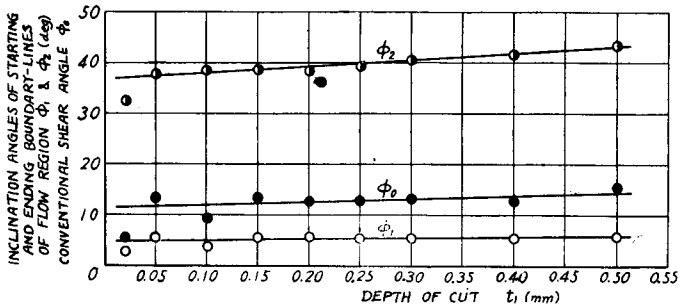

(c) Inclination Angles of Starting and Ending Boundary-Lines of Flow Region, and Conventional Shear Angle

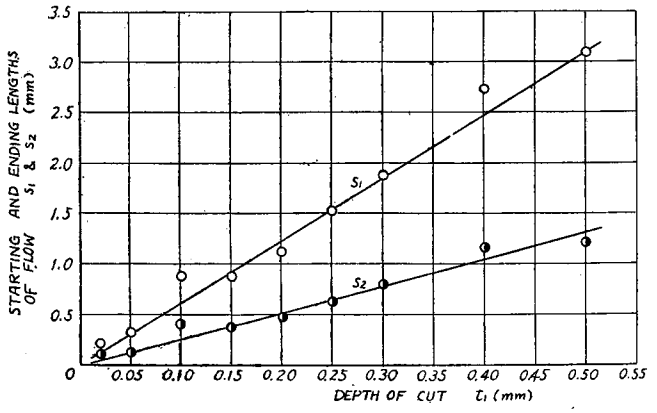

(e) Starting and Ending Lengths of Flow

Fig. 16. The Calculated Quantities for Lead in Relation to Depth of Cut.
(Cutting Conditions: Cutting Velocity 5.2 m/min, Rake Angle 0°)

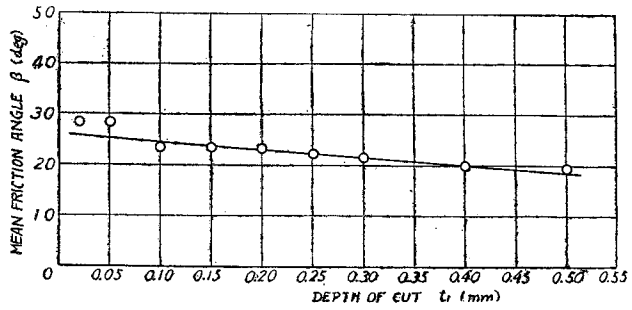

(b) Mean Friction Angle

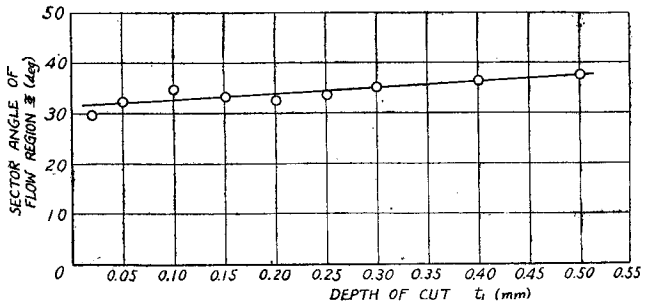

(d) Sector Angle of Flow Region

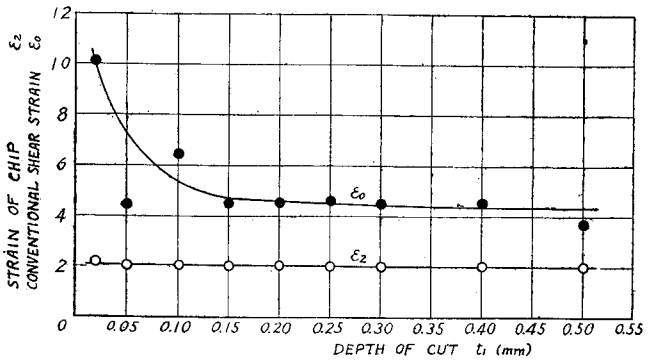

(f) Strain of Chip, and Conventional Shear Strain

Fig. 16 (Continued).

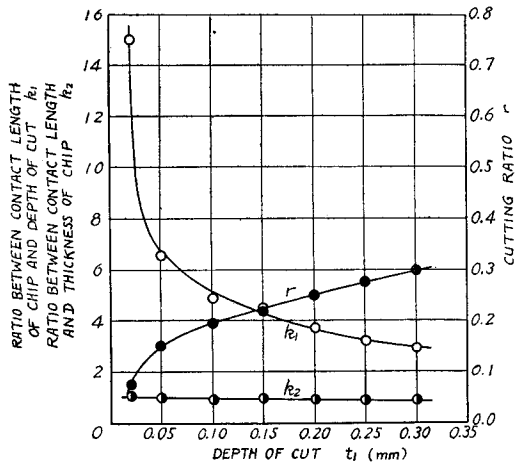

(a) Cutting Ratio, Ratio between Contact Length of Chip and Depth of Cut, and Ratio between Contact Length and Thickness of Chip

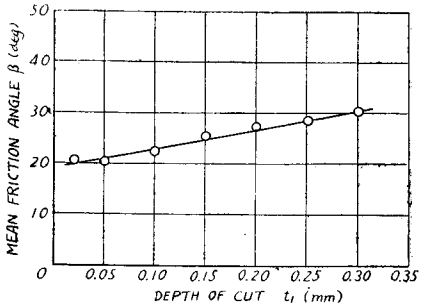

(b) Mean Friction Angle

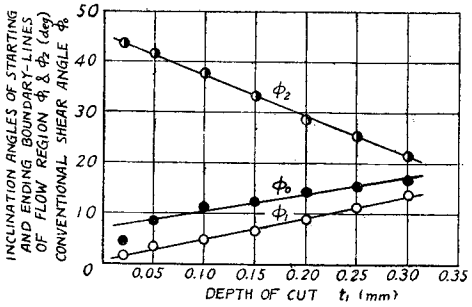

(c) Inclination Angles of Starting and Ending Boundary-Lines of Flow Region, and Conventional Shear Angle

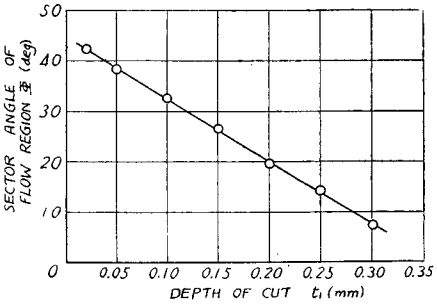

(d) Sector Angle of Flow Region

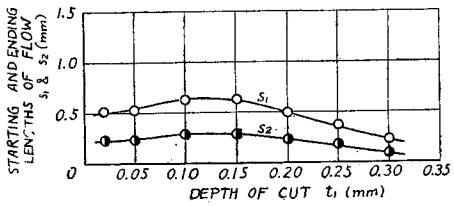

(e) Starting and Ending Lengths of Flow

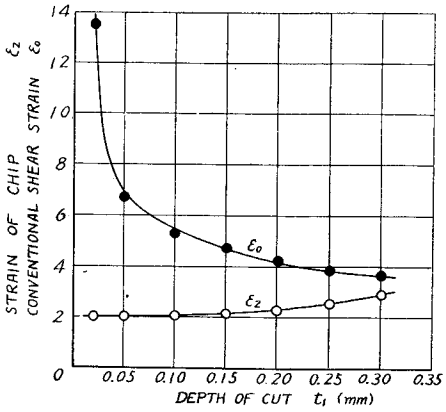

(f) Strain of Chip, and Conventional Shear Strain

Fig. 17. The Calculated Quantities for Brass in Relation to Depth of Cut.
(Cutting Conditions: Cutting Velocity 5.2 m/min, Rake Angle 0°)

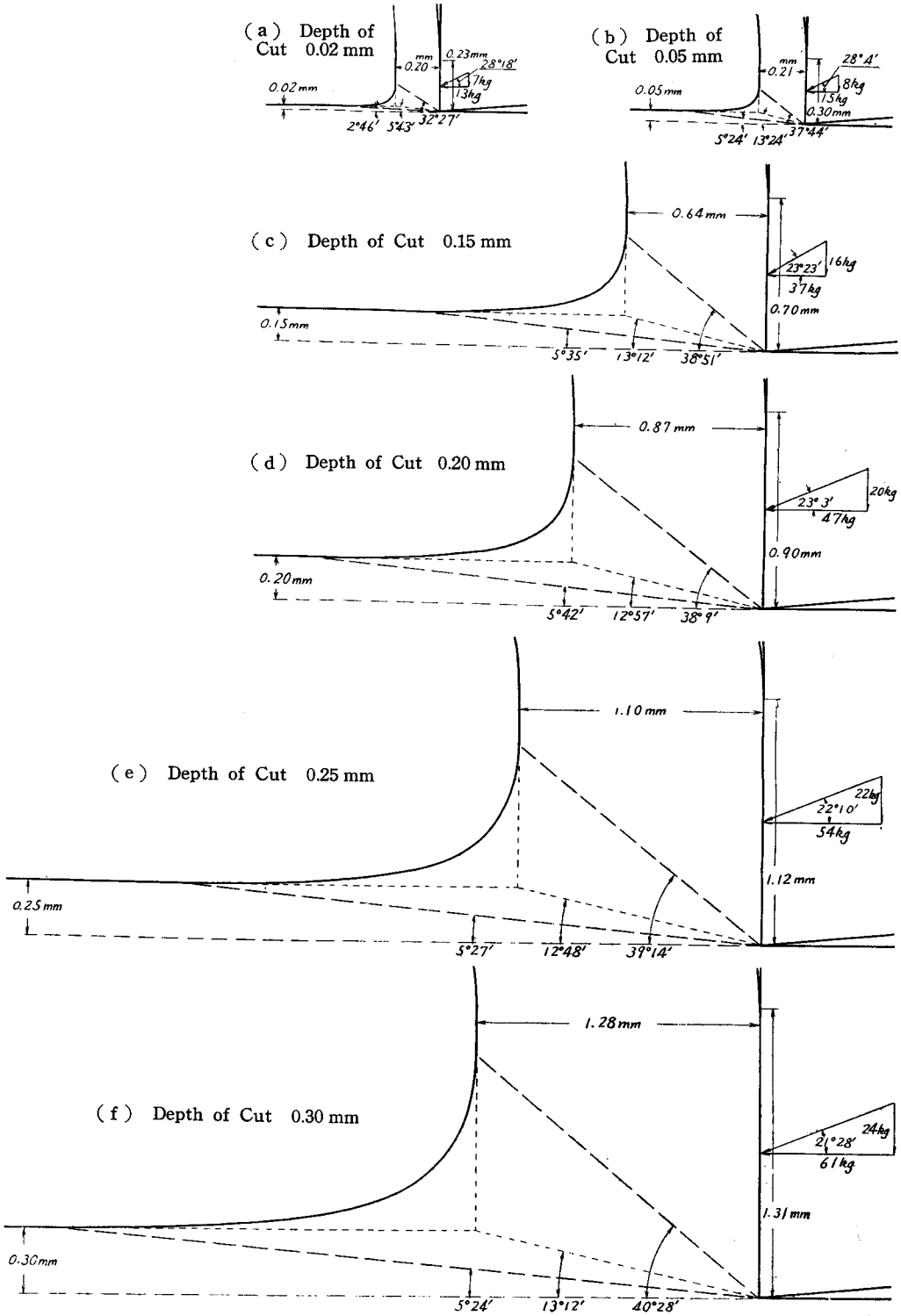

Fig. 18. The Cutting Schema for Lead in Relation to Depth of Cut.
(Cutting Conditions: Cutting Velocity 5.2m/min, Rake Angle 0°)

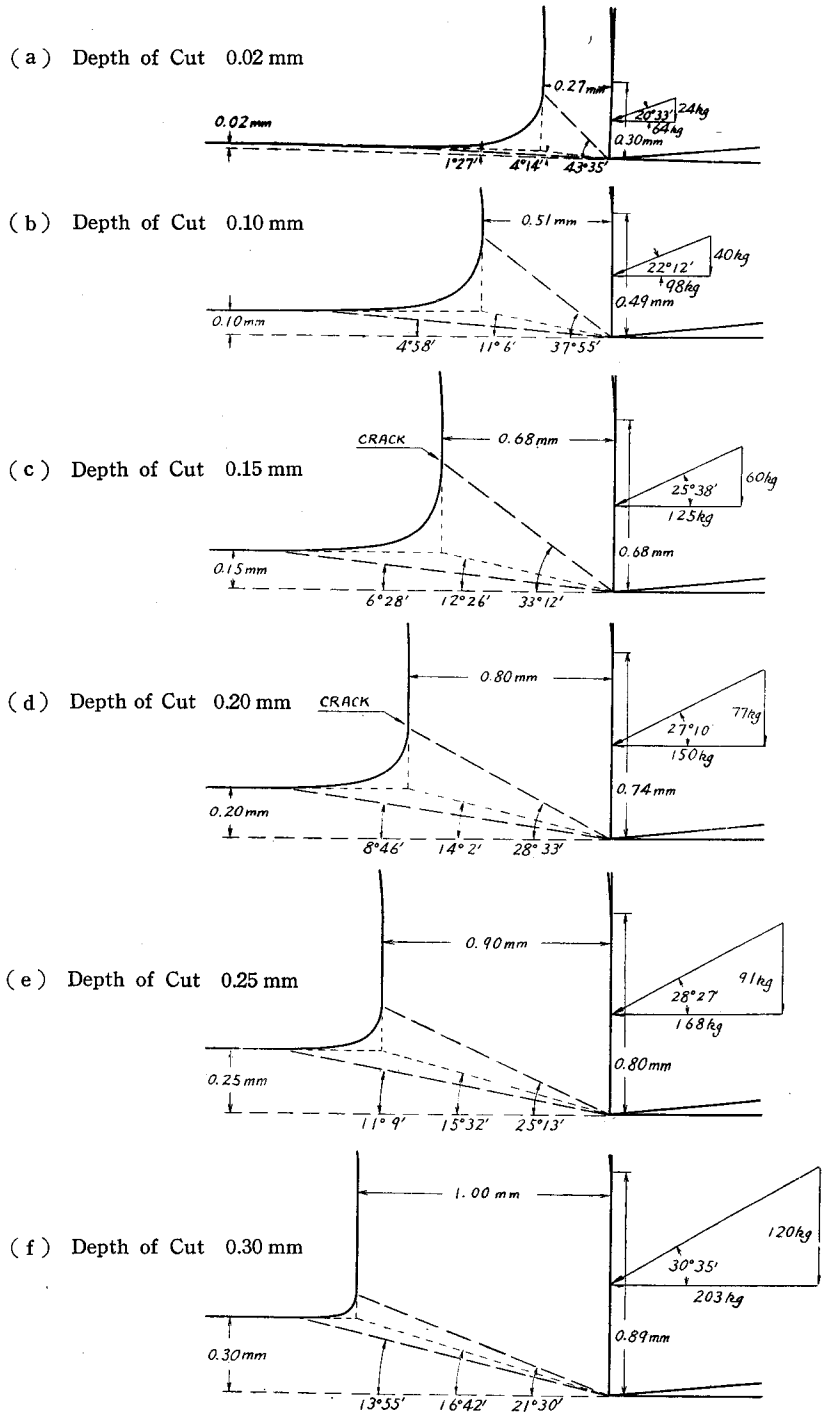

Fig. 19. The Cutting Schema for Brass in Relation to Depth of Cut.
(Cutting Conditions: Cutting Velocity 5.2 m/min, Rake Angle 0°)

is smaller for the cutting process with a flow region. Such cutting mechanism with a flow region seems to be more reasonable than the conventional cutting mechanism with a single shear plane from the standpoint not only of smooth movement of a metal-particle but also of strain and strain rate.

6. Conclusions

The orthogonal cutting mechanism based on the transitional "flow region" concept, instead of the conventional single shear plane, is analyzed theoretically in the case in which the simple continuous chip is produced under the assumption of a perfectly plastic solid, and the experimental data for lead and bass are discussed. This leads to the following conclusions:

(i) The theoretical expressions for the cutting process with a flow region can be applied to a wide range of cutting conditions. The starting boundary-line of flow region is situated under the conventional shear line, and the ending boundary-line above it.

(ii) The theoretical expressions are not inconsistent when applied to the cases of quasi-continuous and discontinuous types of chip. It appears from this fact that there is no essential difference between the formation mechanism of continuous and discontinuous types of chip, and that the type of chip produced depends simply on whether or not the shearing stress and strain at the ending boundary-line of flow region are smaller than the breaking limit.

(iii) The inclination angles of starting and ending boundary-lines and the sector angle of flow region increase with rake angle, and this fact has a bearing upon the increase tendency of the mean friction angle on the tool face with an increase of rake angle.

(iv) The inclination angle of starting boundary-line of flow region increases with depth of cut. On the other hand, the inclination angle of ending boundary-line and, hence, the sector angle of flow region increase for lead, but decrease for brass with an increase of depth of cut—which has a connection with the decrease tendency of the mean friction angle on the tool face for lead and its increase tendency for brass with an increase of depth of cut.

(v) The strain of chip based on the cutting process with a flow region decreases with an increase of rake angle, and has a tendency to decrease slightly for lead and increase gradually for brass with an increase of depth of cut. Moreover, it is much smaller than the conventional shear strain based on the cutting process with a single shear plane, which also means that the rate of strain for the cutting process with a flow region becomes less. The flow region concept seems to be more rational from this point of view also.

(vi) The ratio between contact length of chip and depth of cut varies widely with cutting conditions, while the ratio between contact length and thickness of chip does not vary and it is almost always nearly one.

Bibliography

1) Okushima, K. & Hitomi, K.: On the Cutting Mechanism for Soft Metals, *Memoirs of the Faculty of Engineering, Kyoto University, Japan*, vol. 19 (1957), pp. 135–166.
2) Finnie, I. & Shaw, M. C.: The Friction Process in Metal Cutting, *Trans. ASME*, vol. 78 (1956), pp. 1649–1657.
3) Sata, T. & Mizuno, M.: Friction Process on Cutting Tool and Cutting Mechanism, *Journal of the Scientific Research Institute, Japan*, vol. 49 (1955), pp. 163–174.
4) Meyer, A. W. & Archibald, F. R.: Carbide Milling of Steel, *Mechanical Engineering*, vol. 67 (1945), pp. 659–667.
5) Archibald, F. R.: Analysis of the Stresses in a Cutting Edge, *Trans. ASME*, vol. 78 (1956), pp. 1149–1154.
6) Creveling, J. H., Jordan, T. F. & Thomsen, E. G.: Some Studies of Angle Relationships in Metal Cutting, *Trans. ASME*, vol. 79 (1957), pp. 127–138.
7) Takeyama, H.: Cutting Speed Effect in Metal Machining — Effect of Chip-Tool Contact Area (Part 1), *Journal of the Society for Precision Mechanics of Japan*, vol. 22 (1956), pp. 108–113.
8) Okushima, K. et al.: Wire Resistance Type Three-Component Tool Dynamometer, *Transactions of the Japan Society of Mechanical Engineers*, vol. 21 (1955), pp. 709–711.